Supplementary material

to

"Electrical conductivity fluctuations as a tracer to determine time-dependent transport characteristics in hyporheic sediments"

JONAS L. SCHAPER,[1]* OLAF A. CIRPKA[1] JOERG LEWANDOWSKI[2,3] AND CHRISTIANE ZARFL,[1]

*Corresponding author: Jonas L. Schaper, jonas.schaper@uni-tuebingen.de, Center for Applied Geoscience, Room 4U12 Eberhard Karls University of Tübingen, Schnarrenbergstr. 94-96, D-72076 Tübingen

Content: Number of pages: 1, number of figures: 14, number of tables 1, number of sections: 4

[1] Department of Geosciences, Eberhard Karls University of Tübingen, Tübingen, 72076, Germany
[2] Department Ecohydrology and Biogeochemistry, Leibniz-Institute of Freshwater Ecology and Inland Fisheries, Berlin, 12587, Germany
[3] Geography Department, Humboldt University Berlin, Berlin, 12489, Germany

Contents

1 Model performance and effects of parameter regularization

Table SI-1: Optimal weighting factors and mean root mean squared error (RMSE), apparent longitudinal dispersivity (α), apparent porewater velocity (v) and electrical conductivity offset calculated from all model realizations computed during posterior sampling for different staging posts per day. Weights are considered optimal along the L-curve where its curvature was the highest. SD = standard deviation

Data set	optimal weigth	staging posts	EC offset	v	α	RMSE ± 2SD
		d^{-1}	$\mu S\ cm^{-1}$	$cm\ h^{-1}$	cm	$\mu S\ cm^{-1}$
River Ammer	100000	8	-22 ± 7	1.16 ± 1.53	8.9 ± 0.2	6.11 ± 0.07
River Ammer	100000	4	-24 ± 8	1.10 ± 1.63	8.3 ± 0.2	7.16 ± 0.06
River Ammer	100000	2	-25 ± 8	1.04 ± 1.29	8.8 ± 0.2	9.03 ± 0.03
River Ammer	100000	1	-26 ± 8	0.97 ± 1.00	8.6 ± 0.2	10.16 ± 0.03
River Erpe, 2016	10000	8	-6 ± 4	2.68 ± 1.30	1.8 ± 0.0	2.35 ± 0.23
River Erpe, 2016	10000	4	-6 ± 3	2.53 ± 1.19	2.0 ± 0.0	3.25 ± 0.13
River Erpe, 2016	10000	2	-3 ± 4	2.59 ± 1.45	2.3 ± 0.1	4.81 ± 0.15
River Erpe, 2016	10000	1	1 ± 3	2.12 ± 1.17	2.8 ± 0.1	7.06 ± 0.05
River Erpe, 2019	100000	8	3 ± 12	2.81 ± 0.97	1.0 ± 0.0	2.46 ± 0.19
River Erpe, 2019	100000	4	3 ± 12	2.86 ± 0.97	1.1 ± 0.0	2.60 ± 0.16
River Erpe, 2019	100000	2	3 ± 12	2.86 ± 0.91	1.1 ± 0.0	3.15 ± 0.10
River Erpe, 2019	100000	1	3 ± 12	2.77 ± 0.95	1.1 ± 0.0	3.32 ± 0.09
River Sturt	10000	8	57 ± 12	2.13 ± 2.05	1.4 ± 0.2	1.64 ± 0.12
River Sturt	10000	4	57 ± 13	1.96 ± 2.05	1.3 ± 0.2	1.77 ± 0.10
River Sturt	10000	2	56 ± 11	1.63 ± 1.79	2.0 ± 0.2	2.66 ± 0.09
River Sturt	10000	1	56 ± 10	1.68 ± 0.93	1.9 ± 0.2	3.07 ± 0.04

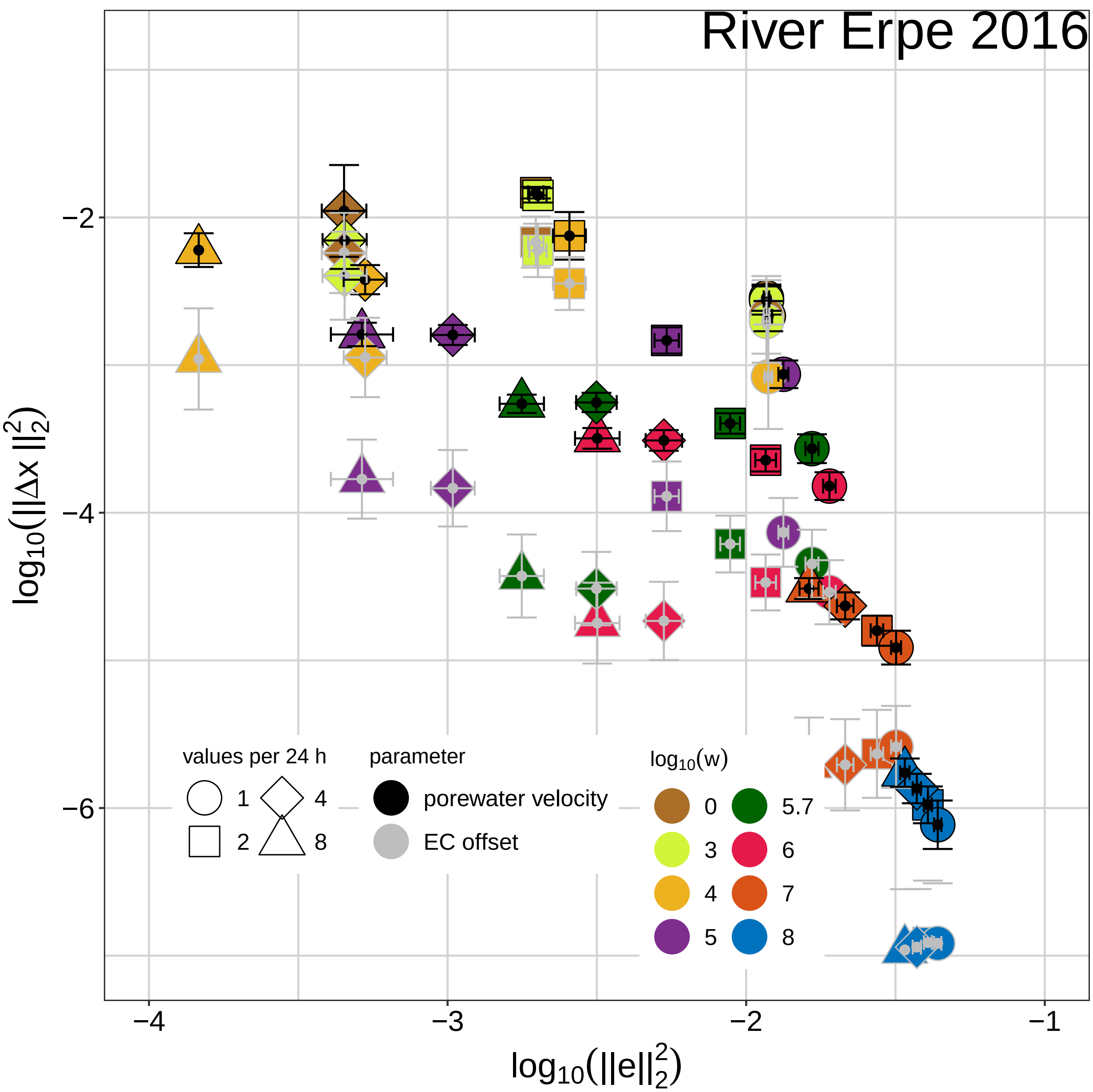

Figure SI-1: L-curve, i.e., a plot the decadic logarithm of the squared Euclidian norm of the model residuals, $log_{10}(\|e\|_2^2)$ versus the squared Euclidian norm of the consecutive difference of parameter values, $log_{10}(\|\delta x\|_2^2)$, for all model runs conducted using the River Erpe 2016 dataset. The regularization weights $w_v(h^2m^{-2})$ for porewater velocity and $w_o(cm^2\mu S^{-2})$ for EC offset were varied (8 colors). For porewater velocity, one, two, four and eight staging posts d^{-1} were used while the temporal resolution of the EC offset was one staging post per day. Weights are considered optimal along the L-curve where its curvature was the highest (i.e., $w_o = w_v = 10^4$ for eight staging posts d^{-1}).

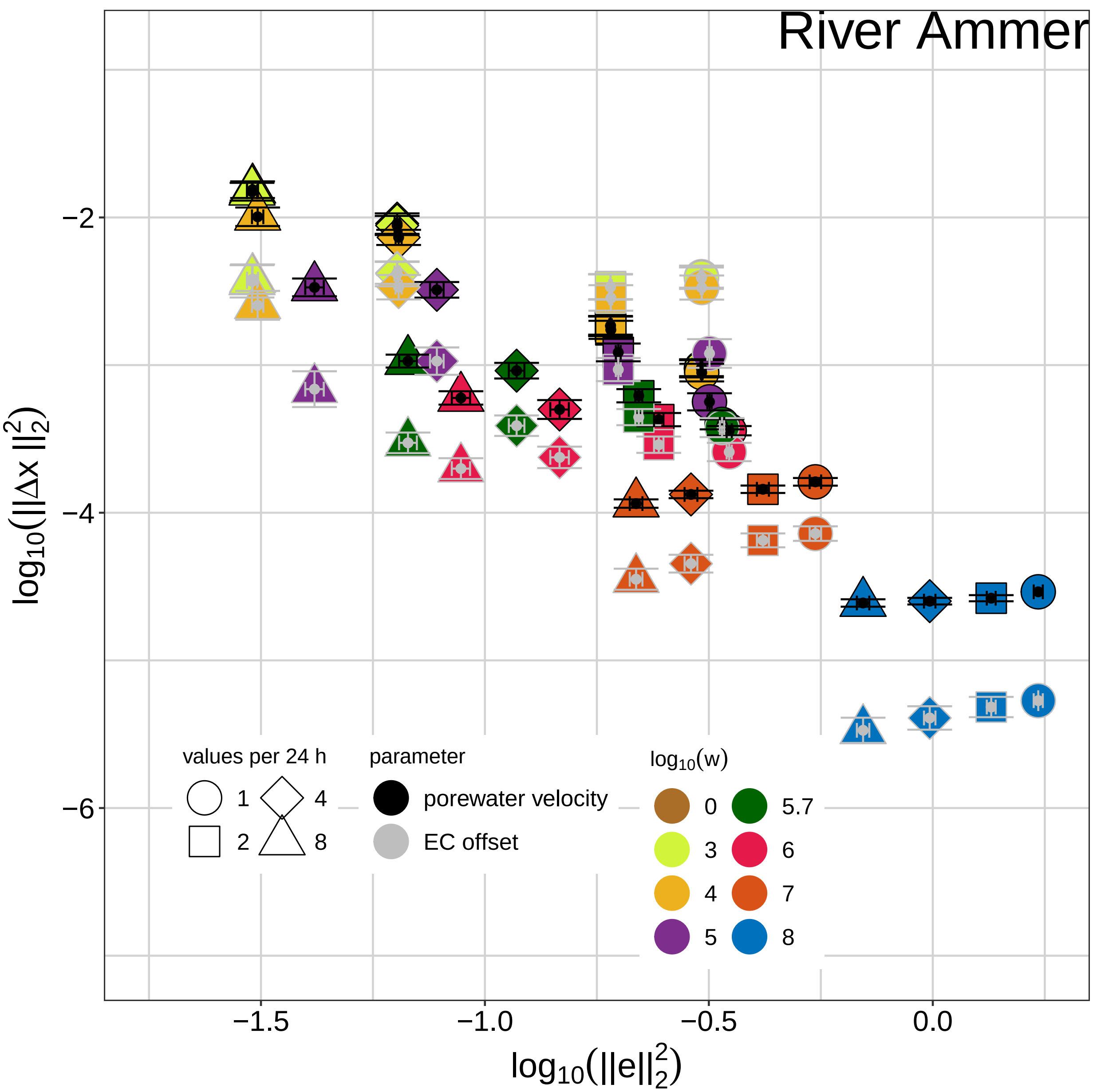

Figure SI-2: L-curve, i.e., a plot the decadic logarithm of the squared Euclidian norm of the model residuals, $log_{10}(\|e\|_2^2)$ versus the squared Euclidian norm of the consecutive difference of parameter values, $log_{10}(\|\delta x\|_2^2)$, for all model runs conducted using the River Ammer dataset. The regularization weights $w_v(h^2m^{-2})$ for porewater velocity and $w_o(cm^2\mu S^{-2})$ for EC offset were varied (8 colors). For porewater velocity, one, two, four and eight staging posts d^{-1} were used while the temporal resolution of the EC offset was one staging post per day. Weights are considered optimal along the L-curve where its curvature was the highest (i.e., $w_o = w_v = 10^5$ for eight staging posts d^{-1}).

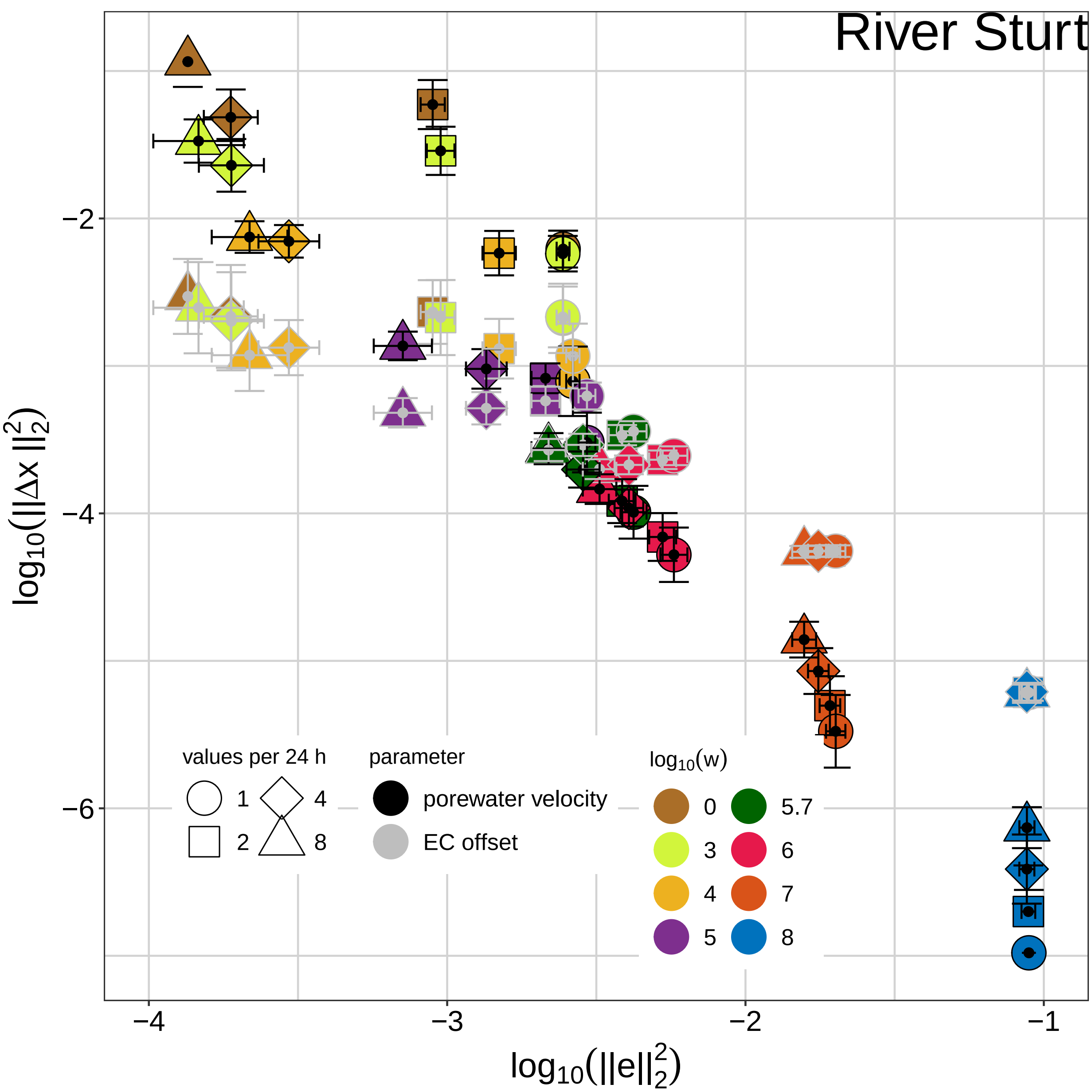

Figure SI-3: L-curve, i.e., a plot the decadic logarithm of the squared Euclidian norm of the model residuals, $log_{10}(\|e\|_2^2)$ versus the squared Euclidian norm of the consecutive difference of parameter values, $log_{10}(\|\delta x\|_2^2)$, for all model runs conducted using the Sturt River dataset. The regularization weights $w_v(h^2m^{-2})$ for porewater velocity and $w_o(cm^2\mu S^{-2})$ for EC offset were varied (8 colors). For porewater velocity, one, two, four and eight staging posts d^{-1} were used while the temporal resolution of the EC offset was one staging post per day. Weights are considered optimal along the L-curve where its curvature was the highest (i.e., $w_o = w_v = 10^4$ for eight staging posts d^{-1}).

2 Measured and modelled time series

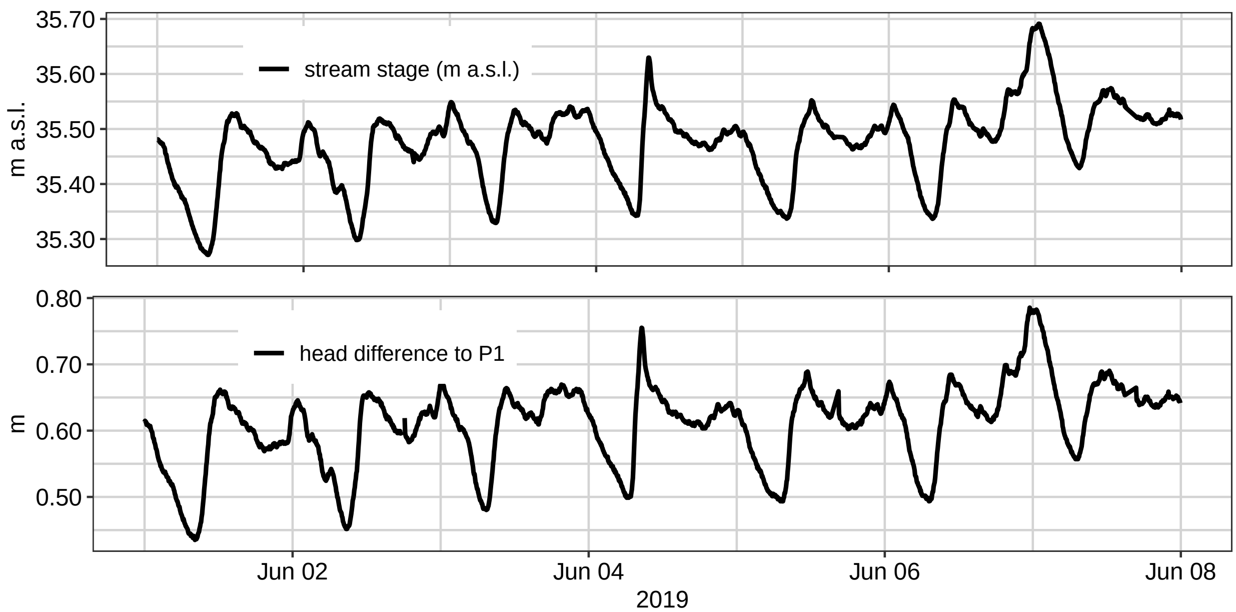

Figure SI-4: Stream stage (upper panel) and head difference between stream stage and the groundwater level measured approx. 3 m away from the stream edge (lower panel).

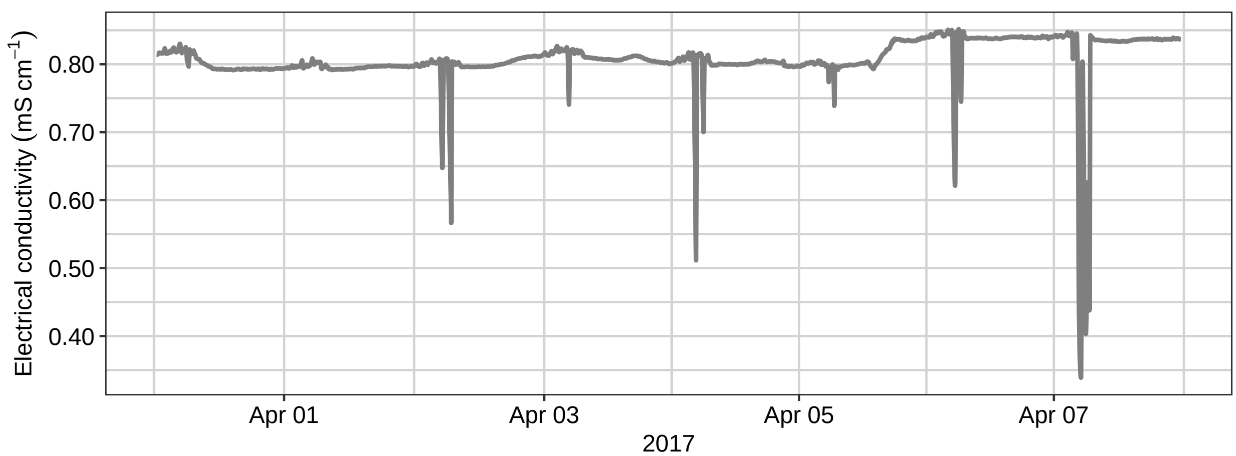

Figure SI-5: Measured time series of electrical conductivity approximately 100 m downstream of the Heathfield wastewater treatment plant (South Australia) discharging into the Sturt River.

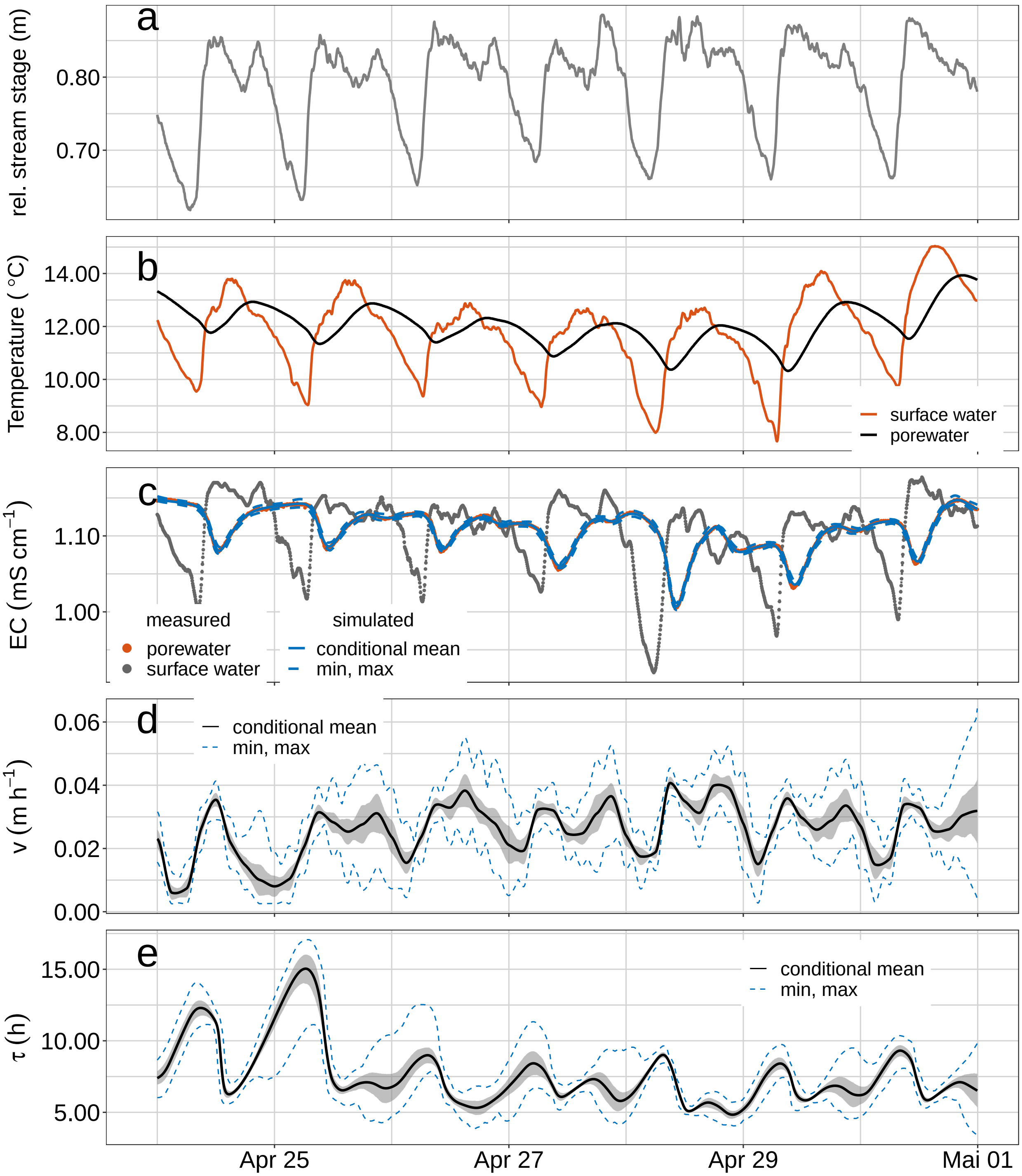

Figure SI-6: a) Stream stage variations relative to CTD diver installation depth in the surface water b) measured time series of surface water temperature c) measured (dots) and modeled (lines) time series of electrical conductivity in the River Erpe 2016 d) measured and modeled time series of apparent porewater velocity v and e) mean advective travel time τ from surface water to the sediment depth of the logger. Grey areas denote one standard deviation around the conditional mean calculated from all accepted model realizations during posterior sampling.

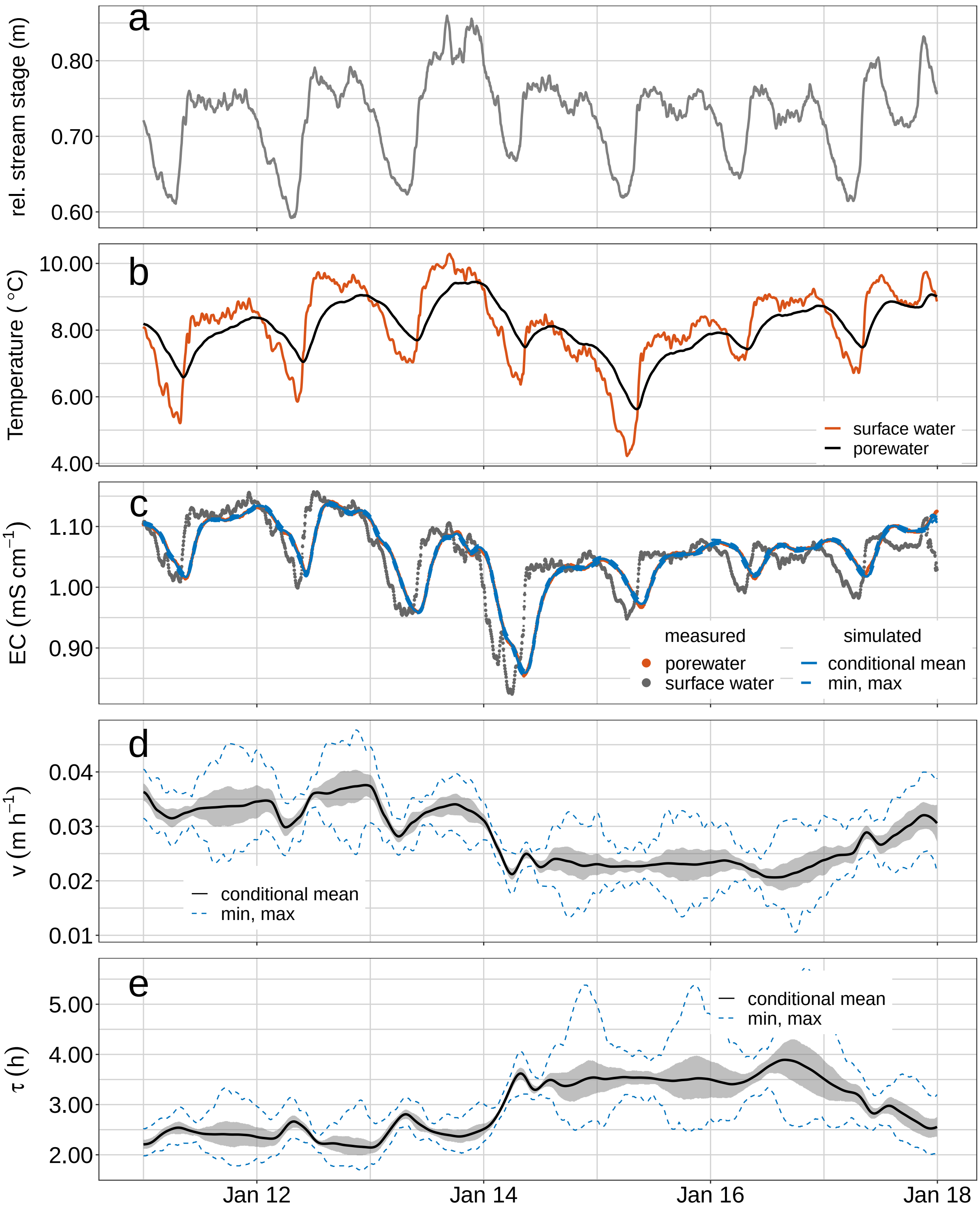

Figure SI-7: a) Stream stage variations relative to CTD diver installation depth in the surface water b) measured time series of surface water temperature c) measured (dots) and modeled (lines) time series of electrical conductivity in the River Erpe 2019 dataset d) measured and modeled time series of apparent porewater velocity v and e) mean advective travel time τ from surface water to the sediment depth of the logger. Grey areas denote one standard deviation around the conditional mean calculated from all accepted model realizations during posterior sampling.

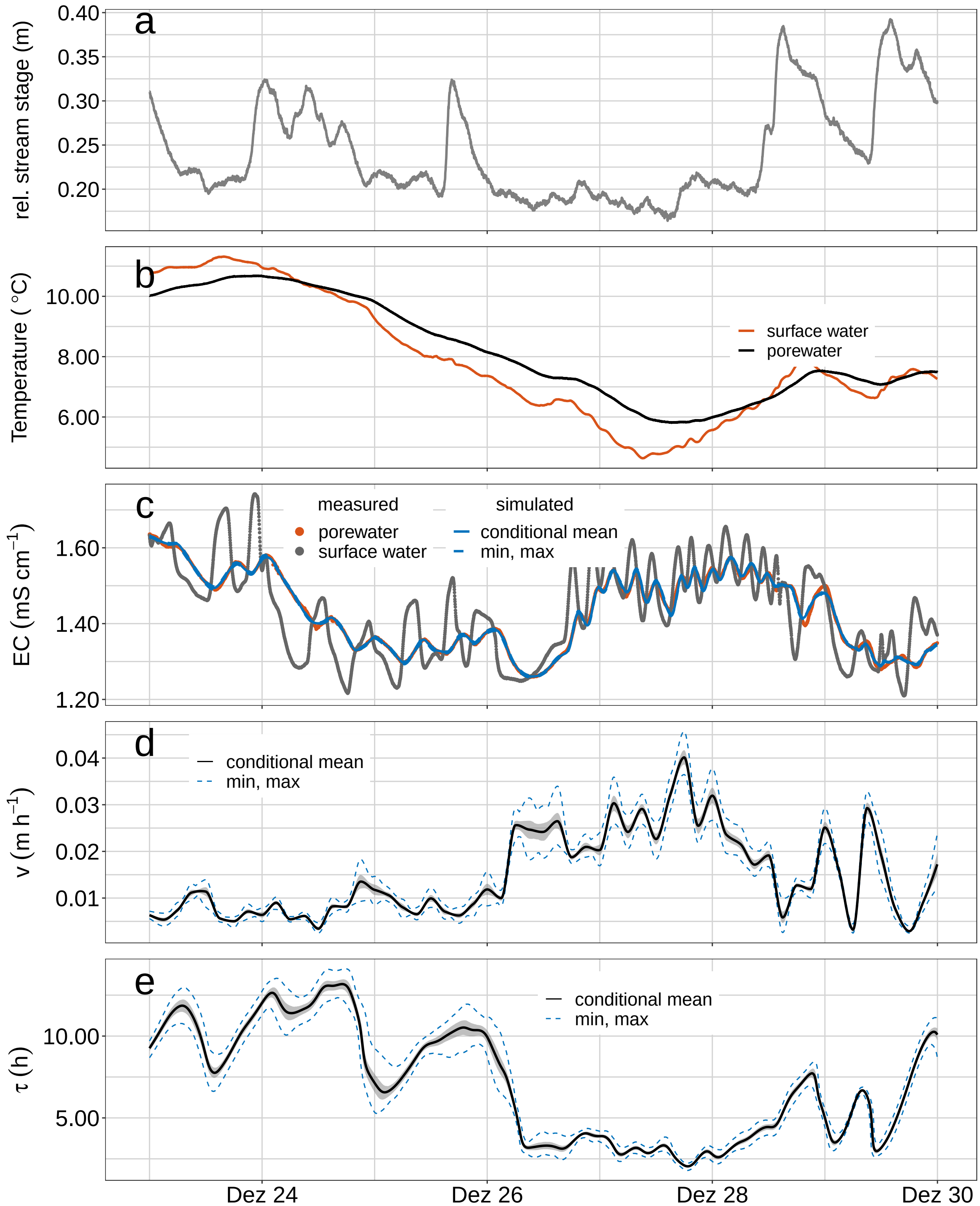

Figure SI-8: a) Stream stage variations relative to CTD diver installation depth in the surface water b) measured time series of surface water temperature c) measured (dots) and modeled (lines) time series of electrical conductivity in the River Ammer dataset d) measured and modeled time series of apparent porewater velocity v and e) mean advective travel time τ from surface water to the sediment depth of the logger. Grey areas denote one standard deviation around the conditional mean calculated from all accepted model realizations during posterior sampling.

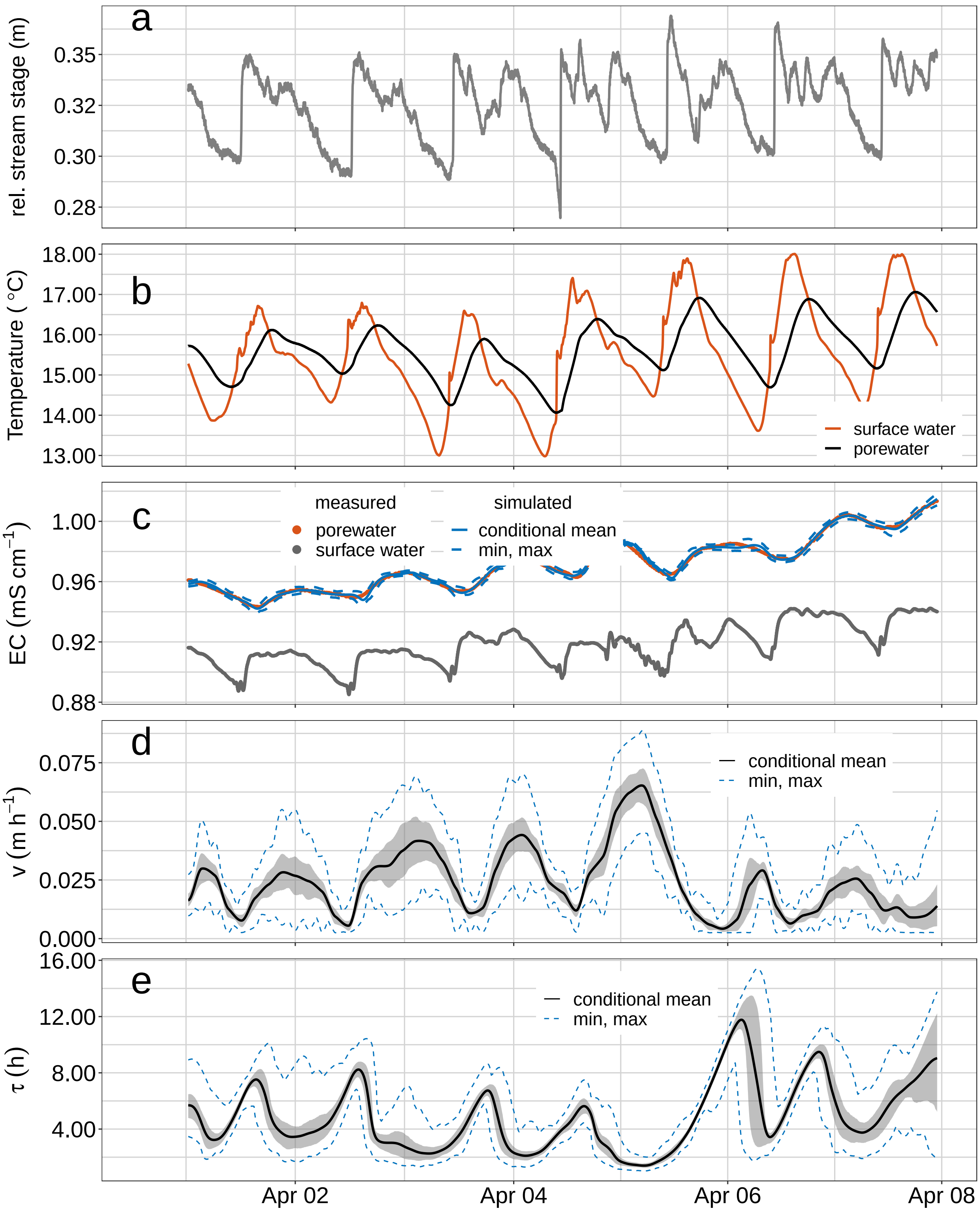

Figure SI-9: a) Stream stage variations relative to CTD diver installation depth in the surface water b) measured time series of surface water temperature c) measured (dots) and modeled (lines) time series of electrical conductivity in the Sturt River dataset d) measured and modeled time series of apparent porewater velocity v and e) mean advective travel time τ from surface water to the sediment depth of the logger. Grey areas denote one standard deviation around the conditional mean calculated from all accepted model realizations during posterior sampling.

3 Time series correlations

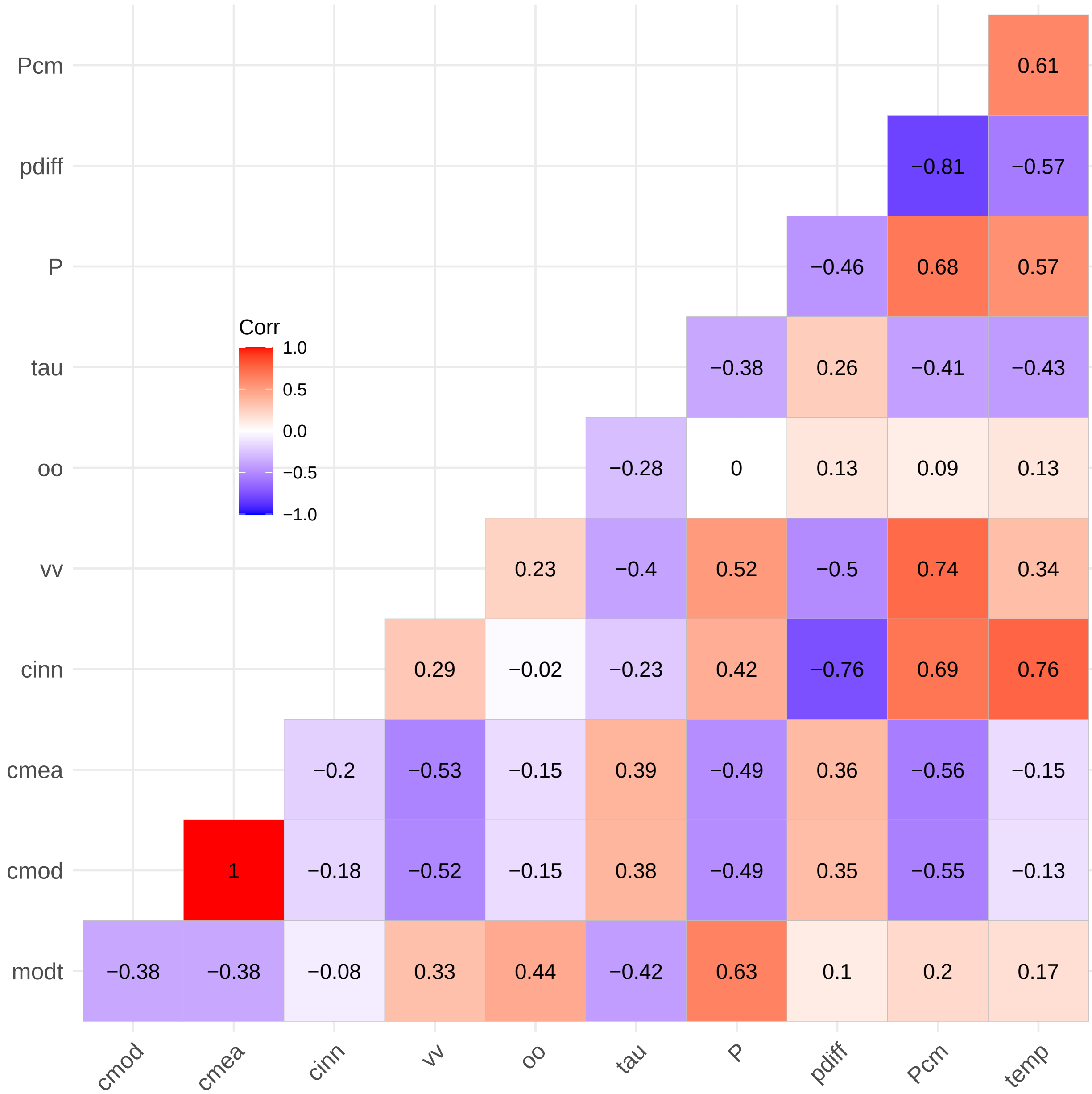

Figure SI-10: Correlation between time series of modelled (EC mod) and measured (EC mea) electrical conductivity in the riverbed sediment, total pressure above the surface water CTD diver (P), height of the water column above the surface water CTD diver (Pcm), pressure difference between the surface water CTD diver and the CTD diver installed in the riverbed sediment, modelled apparent porewater velocity (v) and EC offset (offset), measured temperature in the surface water (temp) and measured electrical conductivity in the surface water for the River Erpe 2016 dataset

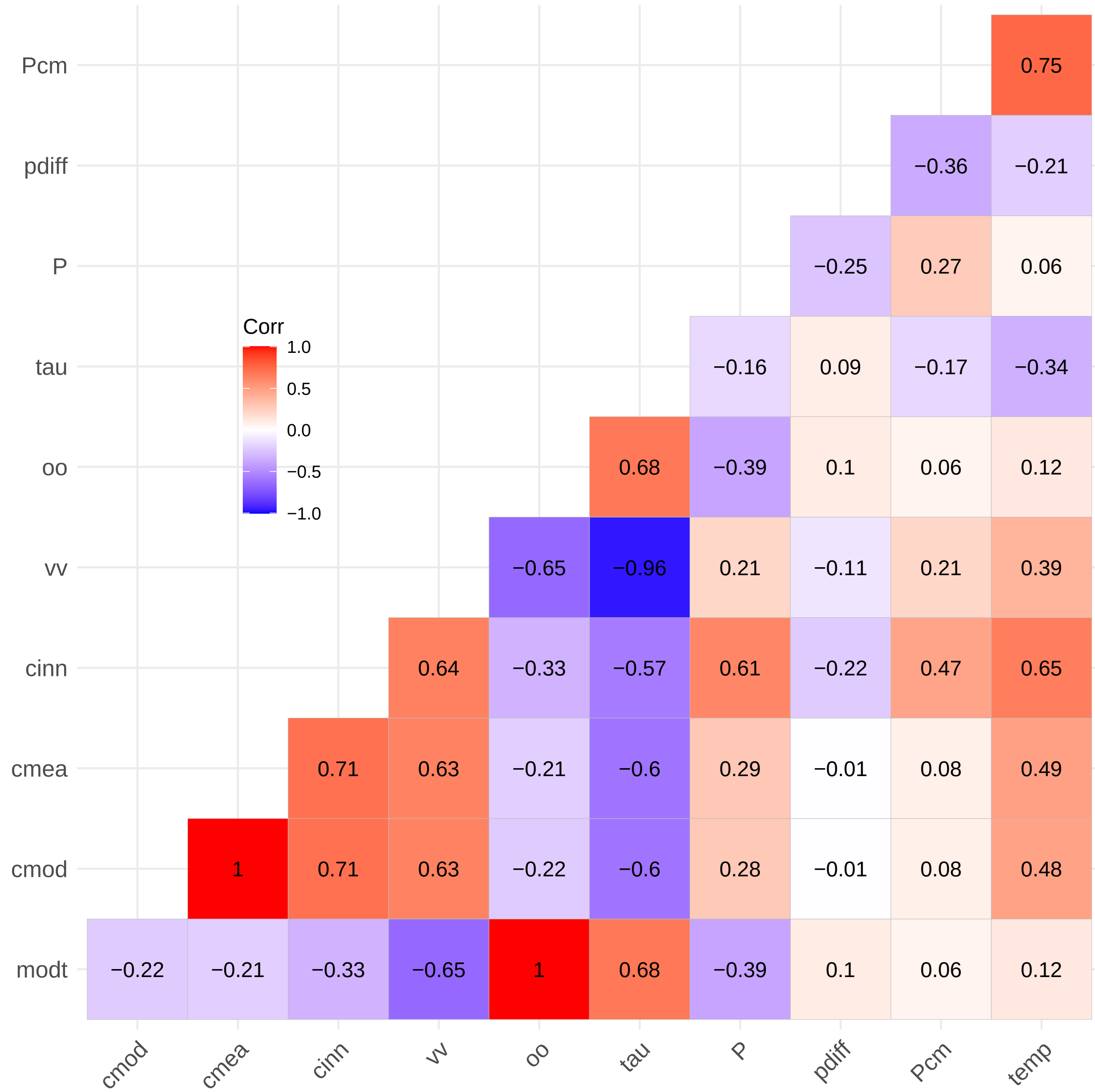

Figure SI-11: Correlation between time series of modeled (EC mod) and measured (EC mea) electrical conductivity in the riverbed sediment, total pressure above the surface water CTD diver (P), height of the water column above the surface water CTD diver (Pcm), pressure difference between the surface water CTD diver and the CTD diver installed in the riverbed sediment, modeled apparent porewater velocity (v) and EC offset (offset), measured temperature in the surface water (temp) and measured electrical conductivity in the surface water for the River Erpe 2019 dataset

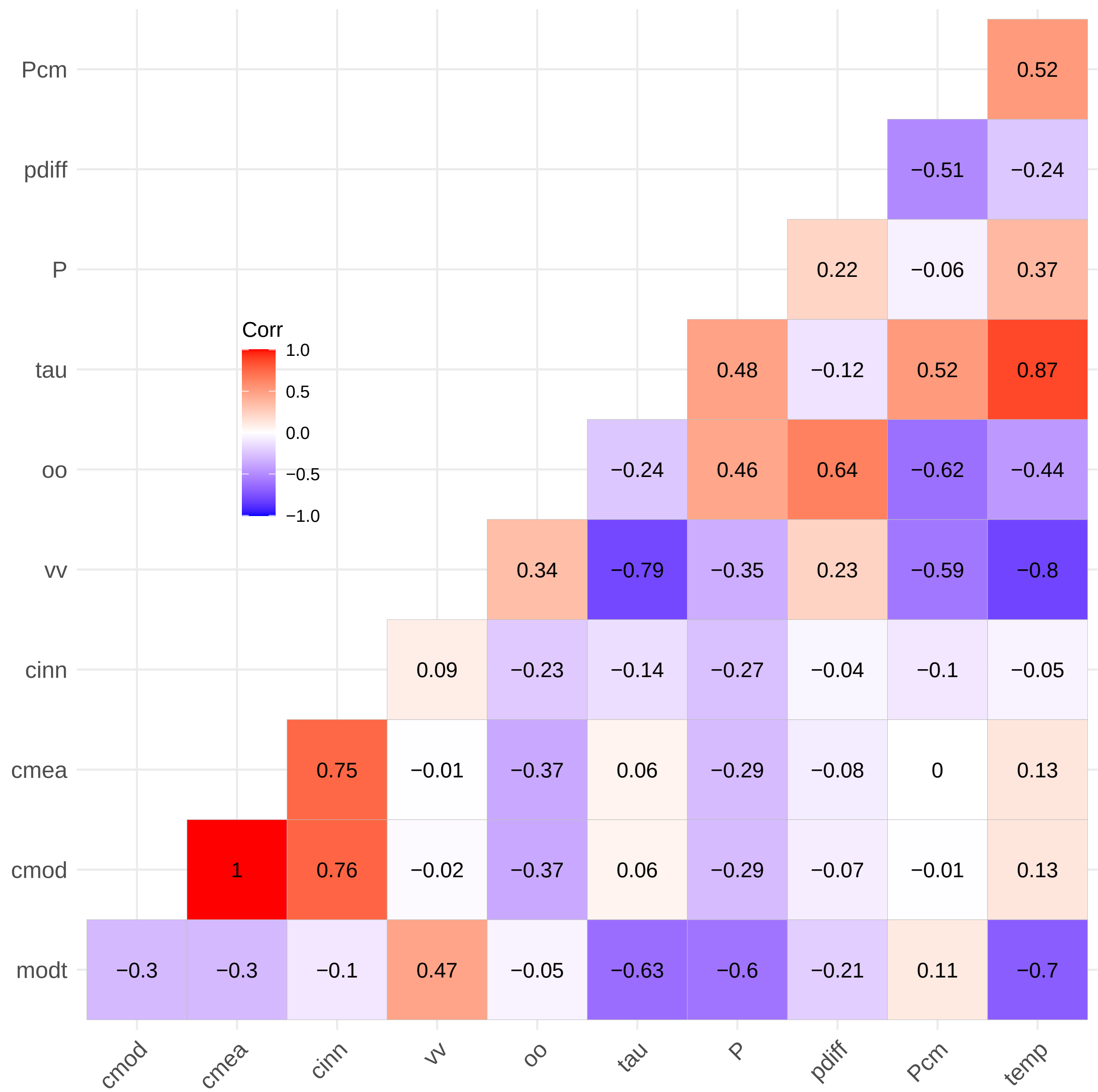

Figure SI-12: Correlation between time series of modeled (EC mod) and measured (EC mea) electrical conductivity in the riverbed sediment, total pressure above the surface water CTD diver (P), height of the water column above the surface water CTD diver (Pcm), pressure difference between the surface water CTD diver and the CTD diver installed in the riverbed sediment, modeled apparent porewater velocity (v) and EC offset (offset), measured temperature in the surface water (temp) and measured electrical conductivity in the surface water for the River Ammer dataset

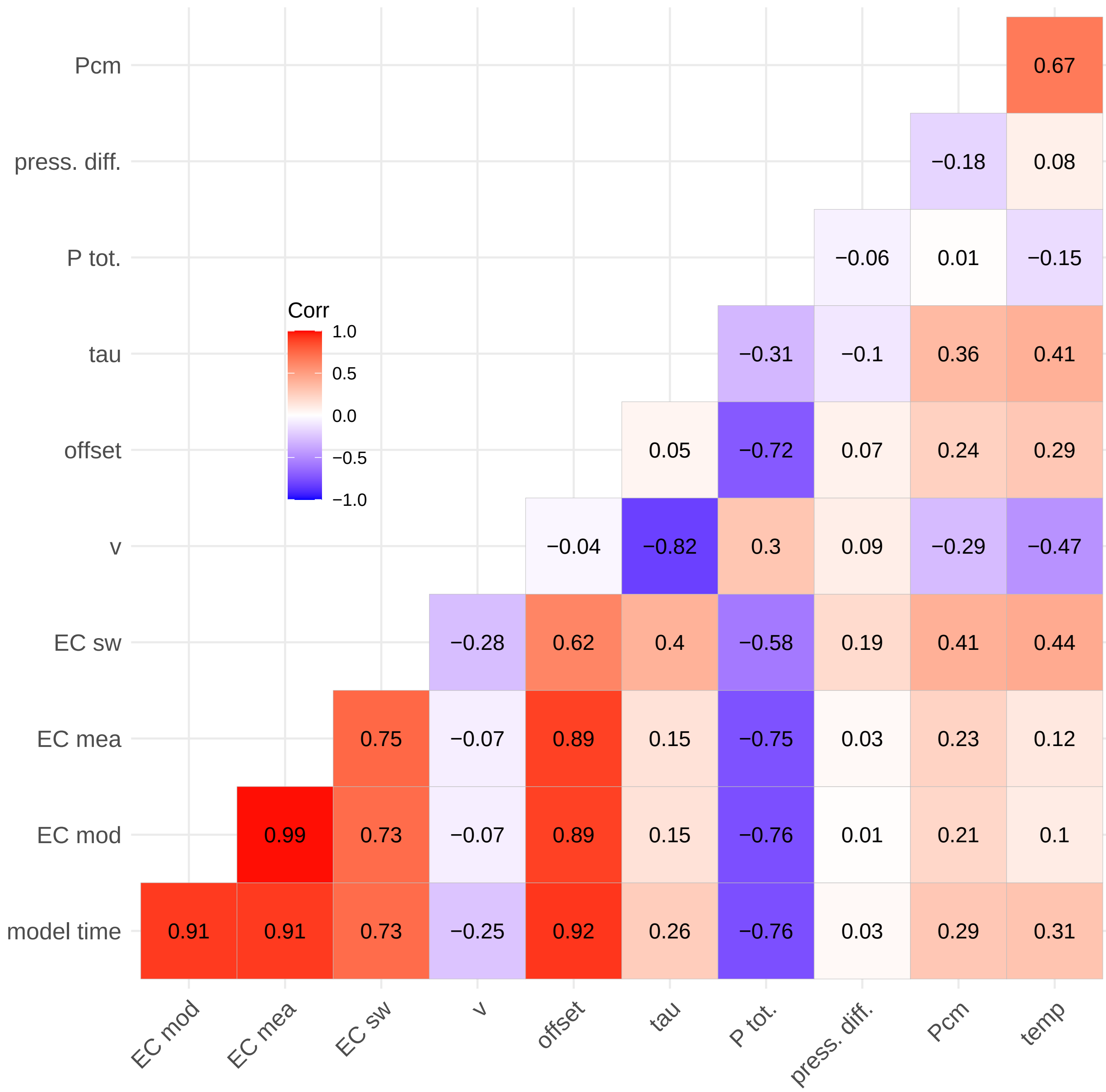

Figure SI-13: Correlation between time series of modeled (EC mod) and measured (EC mea) electrical conductivity in the riverbed sediment, total pressure above the surface water CTD diver (P), height of the water column above the surface water CTD diver (Pcm), pressure difference between the surface water CTD diver and the CTD diver installed in the riverbed sediment, modeled apparent porewater velocity (v) and EC offset (offset), measured temperature in the surface water (temp) and measured electrical conductivity in the surface water for the Sturt River dataset.

4 Time series of EC offset

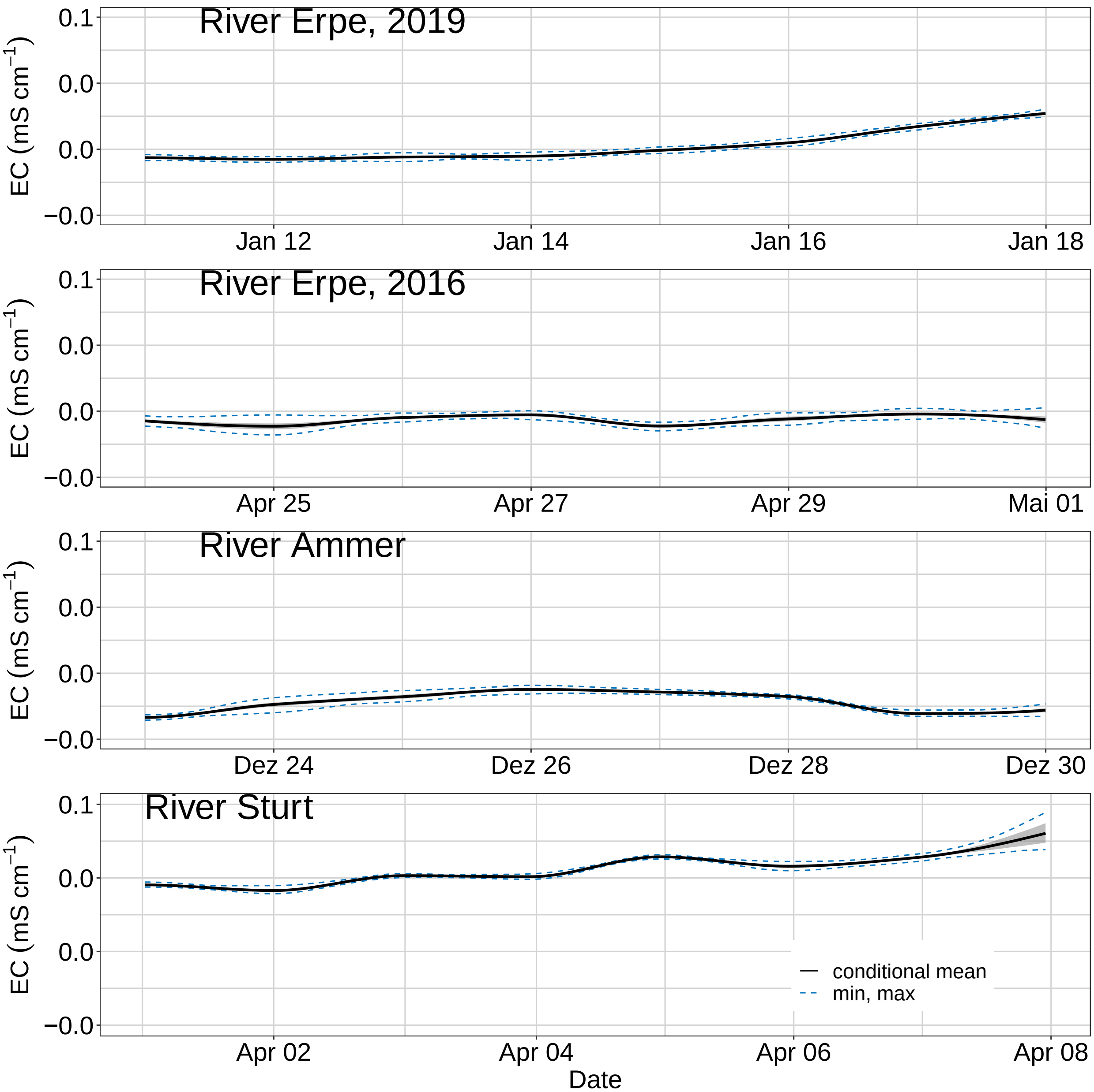

Figure SI-14: Modeled time series of electrical conductivity offset for all four datasets. Grey areas denote one standard deviation around the conditional mean calculated from all accepted model realizations during posterior sampling.